

Mucolipin-3 Regulates Luminal Calcium, Acidification, and Membrane Fusion in the Endosomal Pathway^{*[S]}

Received for publication, July 27, 2010, and in revised form, December 10, 2010. Published, JBC Papers in Press, January 18, 2011, DOI 10.1074/jbc.M110.169185

Benjamin Lelouvier and Rosa Puertollano¹

From the Laboratory of Cell Biology, NHLBI, National Institutes of Health, Bethesda, Maryland 20892

Mucolipin-3 (MCOLN3) is a pH-regulated Ca^{2+} channel that localizes to the endosomal pathway. Gain-of-function mutation in MCOLN3 causes the varitint-waddler (Va) phenotype in mice, which is characterized by hearing loss, vestibular dysfunction, and coat color dilution. The Va phenotype results from a punctual mutation (A419P) in the pore region of MCOLN3 that locks the channel in an open conformation causing massive entry of Ca^{2+} inside cells and inducing cell death by apoptosis. Overexpression of wild-type MCOLN3 produces severe alterations of the endosomal pathway, including enlargement and clustering of endosomes, delayed EGF receptor degradation, and impaired autophagosome maturation, thus suggesting that MCOLN3 plays an important role in the regulation of endosomal function. To understand better the physiological role of MCOLN3, we inhibited MCOLN3 function by expression of a channel-dead dominant negative mutant (458DD/KK) or by knockdown of endogenous MCOLN3. Remarkably, we found that impairment of MCOLN3 activity caused a significant accumulation of luminal Ca^{2+} in endosomes. This accumulation led to severe defects in endosomal acidification as well as to increased endosomal fusion. Our findings reveal a prominent role for MCOLN3 in regulating Ca^{2+} homeostasis at the endosomal pathway and confirm the importance of luminal Ca^{2+} for proper acidification and membrane fusion.

Mucolipin-3 (MCOLN3)² is a cation channel that belongs to the superfamily of transient receptor potential channels. A gain-of-function mutation in MCOLN3 results in the varitint-waddler (Va) phenotype in mice, which is characterized by hearing loss, vestibular dysfunction (circling behavior, head-bobbing, waddling), and coat color dilution (1). Whole cell patch-clamp techniques in cells heterologously expressing MCOLN3 revealed that it is an inwardly rectifying Ca^{2+} -permeable cation channel whose activity is inhibited by acidic extracellular (or luminal) pH and increased by incubation of cells in low Na^+ medium (2–4). The Va phenotype is caused by a point mutation (A419P) in the pore region that locks the channel in an open conformation. It has been suggested that the Va mutant causes massive entry of Ca^{2+} inside cells leading to apoptosis and cell death (2, 4–6).

Endogenous MCOLN3 localizes mainly to intracellular vesicles in hair cells, whereas lower levels of the protein are also observed at the plasma membrane of the stereocilia (1, 7). In HeLa and human fibroblasts, endogenous MCOLN3 was found to be distributed along the endocytic pathway (8, 9). In agreement with these studies, heterologously expressed MCOLN3 co-localizes with early and late endosomes/lysosomes markers in HeLa and ARPE-19 cells (8, 10). Overexpression of MCOLN3 causes severe alterations in the endosomal pathway, including enlargement and clustering of endosomes, delayed epidermal growth factor receptor degradation, and impaired autophagosome maturation, thus suggesting that MCOLN3 plays an important role in the regulation of endosomal function (8, 10).

To gain further insight into the cellular function of MCOLN3, we measured how MCOLN3 regulates several endosomal parameters, including endosomal luminal Ca^{2+} , endosomal pH, and fusion between endosomes. Our data show for the first time that MCOLN3 is required for proper Ca^{2+} homeostasis in the endosomal pathway and that impairment of MCOLN3 function leads to defective endosomal acidification and membrane trafficking.

EXPERIMENTAL PROCEDURES

Measurement of Endosomal Calcium—ARPE-19 cells were grown in Lab-Tek chambered cover glasses (Fisher Scientific). Cells were incubated for 10 min at 37 °C with 100 μM Oregon Green 488 BAPTA-5N and 50 μM Alexa Fluor 555-dextran (Invitrogen). Cells were then washed for 5 min with complete media and incubated in physiological buffer (140 mM NaCl, 4.7 mM KCl, 2 mM CaCl_2 , 1.1 mM MgCl_2 , 50 mM Hepes, 10 mM glucose, pH 7.4) to be processed for confocal microscopy using a LSM 510 confocal system equipped with a live cell imaging chamber (Carl Zeiss, Oberkochen, Germany) directly after rinsing or 1 h after the beginning of the probes internalization. ImageJ (National Institutes of Health) was used to measure the green/red fluorescence ratio of the endosomal compartment. Correlation between the fluorescence ratio and the relative calcium concentration was done by confocal microscopy with an *in situ* calibration procedure in physiological buffer supplemented with 5 μM nigericin and 20 μM ionomycin (Sigma-Aldrich). For calcium concentration between 10 nm and 100 μM , we used isotonic calcium buffers with specific amounts of calcium and calcium ligand (Calbuf 2; World Precision Instrument, Sarasota, FL). For calcium concentration over 500 μM , we prepared physiological buffers with the desired amount of CaCl_2 (without calcium ligand). For zero, we used a physiological buffer with 2 mM EGTA (without calcium).

* This work was supported by the Intramural Research Program of the NHLBI, National Institutes of Health.

[S] The on-line version of this article (available at <http://www.jbc.org>) contains supplemental Methods and Figs. 1–6.

¹ To whom correspondence should be addressed. Tel.: 301-451-2361; Fax: 301-402-1519; E-mail: puertolr@mail.nih.gov.

² The abbreviations used are: MCOLN3, mucolipin-3; Va, varitint-waddler.

Measurement of Endosomal pH—ARPE-19 cells were incubated for 10 min at 37 °C with 500 μM fluorescein isothiocyanate (FITC)-dextran and 50 μM Alexa Fluor 555-dextran. After internalization, cells were washed for 5 min, incubated in physiological buffer, and analyzed by confocal microscopy as described above. Correlation between fluorescence ratio and pH was done by a calibration procedure in a high K^+ buffer (44.7 mM NaCl, 100 mM KCl, 2 mM CaCl_2 , 1.1 mM MgCl_2 , 50 mM Hepes, 10 mM glucose) supplemented with 5 μM nigericin and a pH set up between 4 and 8.

Cell-free Fusion Assay—Two 100-mm dishes of ARPE-19 cells were incubated for 10 min with either 2 $\mu\text{g}/\text{ml}$ Alexa Fluor 488-EGF or 1 $\mu\text{g}/\text{ml}$ Alexa Fluor 555-EGF. Cells were then washed and chased in complete growth medium for 5 min. Internalization was stopped by incubating the cells in cold PBS. Cells were collected and centrifuged at $250 \times g$ for 5 min, resuspended in 400 μl of homogenization buffer (20 mM Hepes, 250 mM sucrose, 2 mM EGTA, 2 mM EDTA, 0.1 mM DTT), homogenized by 15 passages through a 30-gauge needle, and centrifuged for 10 min at $15,000 \times g$. The resulting supernatant were centrifuged for 20 min at $120,000 \times g$ to collect the endosomal fraction and resuspended in 25 μl of homogenization buffer. Endosomal fractions were mixed together with 15 μl of bovine brain cytosol (7.5 mg/ml protein), 5 mM MgATP, 1000 units/ml creatine kinase, 15 mM phosphocreatine, 1 mM DTT, and 90 mM potassium acetate in a total volume of reaction of 100 μl . Controls called “without ATP” were made in absence of ATP and phosphocreatine. After 90 min at 37 °C to allow fusion, 150 μl of 4% formaldehyde solution was added to end the reaction. Endosomes were put directly on acid-washed glass coverslips coated with poly-L-lysine (Sigma). After 20 min of fixation at room temperature, the coverslips were incubated for 2 min with 10% donkey normal serum (Sigma) and 50 mM NH_4Cl in PBS, washed two times with PBS, and mounted onto glass slides with Fluoramount-G (Southern Biotech, Birmingham, AL). Confocal images of labeled endosomes were processed with ImageJ to quantify the proportions of yellow endosomes. Additional procedures are discussed in [supplemental Methods](#).

Statistical Analysis—Data were processed in Excel (Microsoft Corporation, Redmond, WA) then Prism (GraphPad Software, San Diego, CA) to generate curve and bar charts and perform statistical analyses. One-way ANOVA and pairwise post-tests were performed for each dependent variable. $p < 0.05$ was considered statistically significant (*), $p < 0.01$ very significant (**), and $p < 0.001$ extremely significant (***). $p > 0.05$ was considered not significant (NS).

RESULTS AND DISCUSSION

MCOLN3 Regulates Luminal Calcium Concentration at Endosomes—Endocytic vesicles contain high levels of Ca^{2+} when they pinch off from the plasma membrane due to the elevated concentrations of this ion in the extracellular medium. Within 20 min, the concentration of Ca^{2+} in the lumen of endosomes is dramatically reduced because Ca^{2+} release is required to allow efficient endosomal acidification (11). The channel responsible for releasing Ca^{2+} from endosomal compartments remains to be identified. Given the properties of MCOLN3 (*i.e.* Ca^{2+} permeability, localization to the endo-

somal pathway, regulation by pH) we previously suggested that MCOLN3 might mediate release of Ca^{2+} from endosomes (10). Our model predicts that alteration of MCOLN3 function will lead to an increased accumulation of Ca^{2+} in the lumen of endosomes. To assess this possibility, we disrupted MCOLN3 activity by either overexpression of an inactive MCOLN3 mutant or by depletion of endogenous MCOLN3 and then measured the concentration of luminal Ca^{2+} .

All of the experiments were performed in the human retinal pigmented epithelial cell line ARPE-19 (12). There are several reasons to choose this cell type, including the presence of an elaborated endosomal pathway, the expression of endogenous MCOLN3, and the fact that we have previously used ARPE-19 cells to address the distribution of recombinant MCOLN3 and the effect of MCOLN3 overexpression on the endosomal pathway (10).

Luminal Ca^{2+} concentration was measured by fluorescence ratio imaging. Cell-impermeant Oregon Green 488 BAPTA-5N (Ca^{2+} indicator) and Alexa Fluor 555-conjugated dextran (non-sensitive to Ca^{2+}) were simultaneously loaded for 10 min into the endosomal pathway by endocytosis. Cells were then washed and analyzed by confocal microscopy at 20 min or 1 h after the beginning of the loading to monitor luminal Ca^{2+} at the early and late endosomal pathways, respectively (Fig. 1, A and B). The ratio of green (Oregon Green 488 BAPTA-5N) to red (Alexa Fluor 555) fluorescence is indicative of the luminal Ca^{2+} concentration in endocytic vesicles. To determine the correlation between fluorescence ratios and relative Ca^{2+} concentration we constructed a calibration curve by incubating cells with various concentrations of Ca^{2+} or the Ca^{2+} chelator EGTA as described under “Experimental Procedures” (Fig. 1C).

To assess the correct trafficking of our Ca^{2+} probe along the endocytic pathway, we monitored the co-localization of Oregon Green 488 BAPTA-5N with transferrin and dextran as markers for early and late endosomes/lysosomes, respectively. As shown in [supplemental Fig. 1](#), close to 90% (89.1 ± 0.28 S.E.) of the vesicles labeled by Oregon Green also contain transferrin after a 20-min internalization, indicating that the probe is mostly located at early endosomes at this time point. In contrast, after 1-h internalization most Oregon Green ($87\% \pm 0.24$) co-localizes with dextran, thus confirming delivery of the Ca^{2+} probe to late endosomes/lysosomes. We also performed control experiments showing that the Ca^{2+} probe has only a negligible sensitivity to pH ([supplemental Fig. 2](#)).

To address the contribution of MCOLN3 to endosomal Ca^{2+} homeostasis, we prepared an adenovirus expressing an inactive MCOLN3 mutant (MCOLN3 DDKK). The DDKK mutant was generated by mutation of two aspartate residues located at the pore region to lysines (458DD/KK). Patch-clamp experiments confirmed that the MCOLN3 DDKK mutant was inactive (data not shown). Introduction of equivalent mutations in MCOLN1 and MCOLN2 is known to inhibit the channel activity of these proteins (13–15). Moreover, the DDKK mutants seem to sequester endogenous MCOLNs into inactive complexes, thus having a dominant negative effect (13). Quantification of multiple random fields of cells showed that overexpression of MCOLN3 DDKK caused a significant reduction in the release of Ca^{2+} from both early and late endosomes (Fig. 1, D and E).

MCOLN3 Regulates Endosomal Calcium

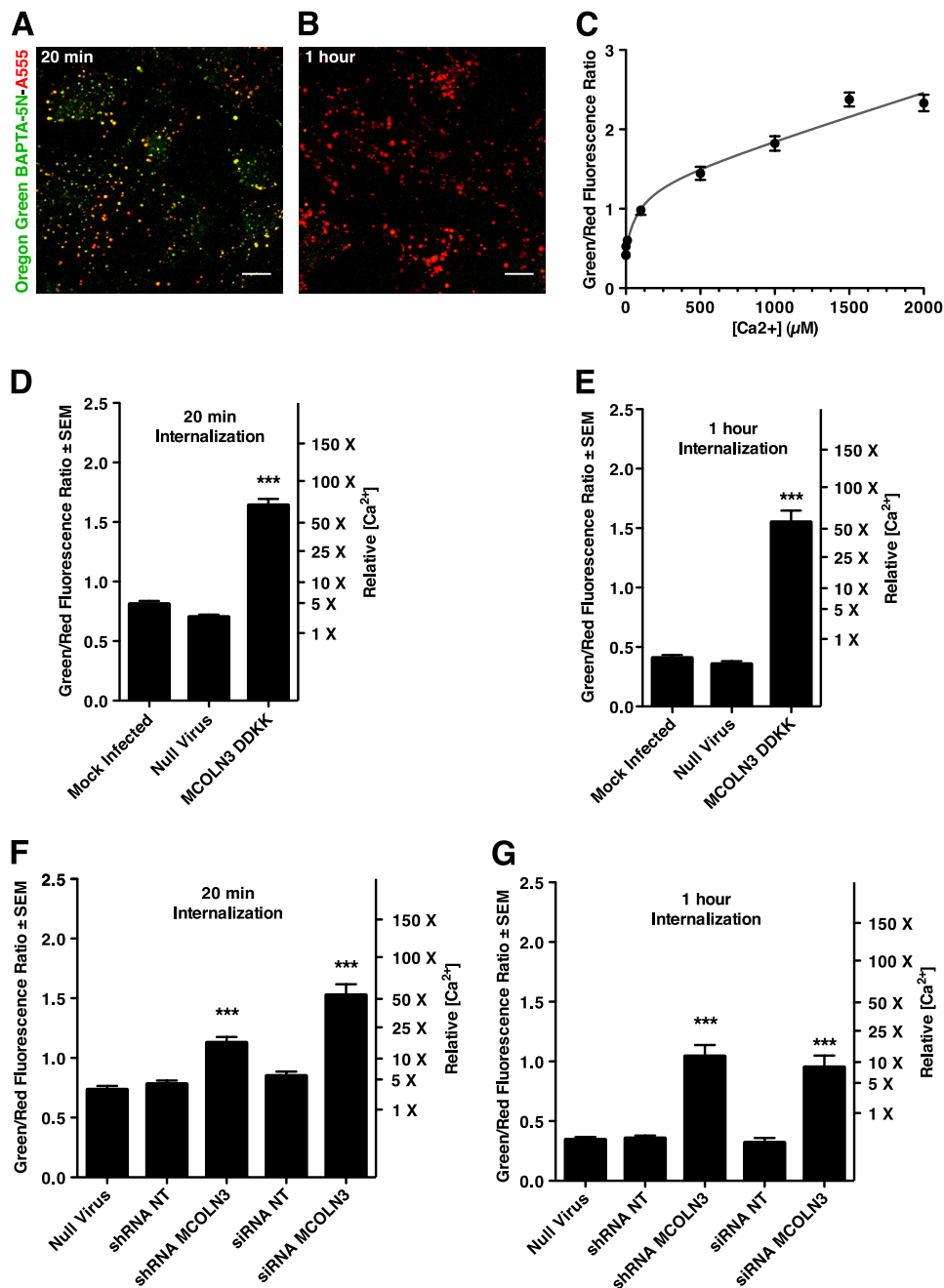


FIGURE 1. Inhibition of MCOLN3 induces accumulation of endosomal Ca²⁺. *A* and *B*, measurement of luminal Ca²⁺ by fluorescence ratio imaging at 20 min (*A*) or 1 h (*B*) after internalization of the probes. Scale bars, 10 μm. *C*, correlation between fluorescence ratio and Ca²⁺ concentration performed by fitting the data to an *in situ* calibration curve (using calcium buffers and nigerin/ionomycin). *D* and *E*, quantification of luminal Ca²⁺ in mock-infected cells and cells infected for 40 h with either a control adenovirus (*Null Virus*) or an adenovirus expressing a MCOLN3 mutant (*MCOLN3 DDKK*) at 20-min (*D*) or 1-h (*E*) internalization. *F* and *G*, endogenous MCOLN3 depleted by either shRNA (*shRNA MCOLN3*) or siRNA (*siRNA MCOLN3*). The endosomal Ca²⁺ was measured after 20-min (*F*) or 1-h (*G*) internalization. A null virus, nontarget siRNA (*siRNA NT*), and nontarget siRNA (*siRNA NT*) were used as controls. Data are presented as -fold increase (*X*) to a reference calcium concentration. Bars represent mean ± S.E. of three independent experiments (***, *p* < 0.001).

Endosomes from cells overexpressing MCOLN3 DDKK showed >10-fold increase in the amount of luminal Ca²⁺ compared with mock-infected cells or cells infected with a control null virus (Fig. 1, *D* and *E*).

To confirm the role of MCOLN3 in the regulation of endosomal Ca²⁺ further, we analyzed the effect of depleting endogenous MCOLN3. Depletion of endogenous MCOLN3 was achieved either by infection with a recombinant adenovirus expressing a shRNA targeted against MCOLN3 or by transfection

with an anti-MCOLN3 siRNA. An 80–90% reduction in the levels of MCOLN3 mRNA was observed in both cases as assessed by quantitative RT-PCR (supplemental Fig. 3). As expected, the concentration of Ca²⁺ in the lumen of endosomes was significantly increased in cells depleted of MCOLN3 (Fig. 1, *F* and *G*). In contrast, the endosomal Ca²⁺ concentration in cells infected with a null virus, a virus expressing a nontargeted shRNA, or in cells transfected with control siRNA did not differ from the untreated cells (Fig. 1, *F* and *G*). Therefore, our results

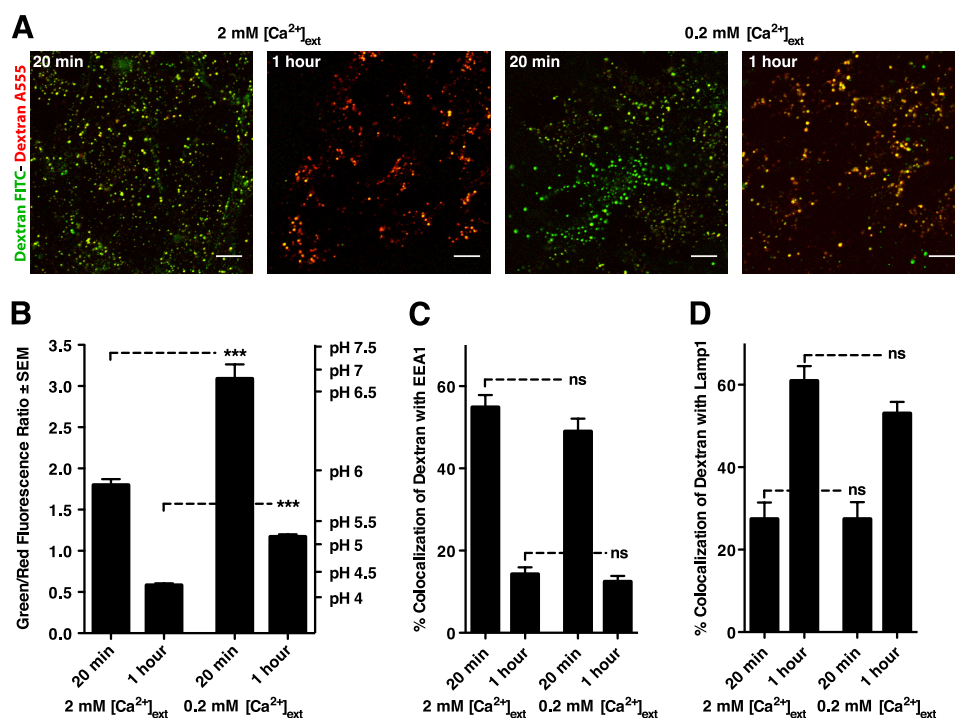


FIGURE 2. Extracellular calcium concentration affects endosomal acidification. *A*, measurement of endosomal pH (20-min internalization) and late endosomal/lysosomal pH (1-h internalization) was performed by confocal microscopy in cells preincubated in buffer with normal (2 mM) or low (0.2 mM) Ca²⁺ concentrations. Scale bars, 10 μ m. *B*, quantification of three independent experiments shows decreased acidification when the extracellular Ca²⁺ is low. ***, $p < 0.001$. *C* and *D*, extracellular Ca²⁺ concentration does not affect co-localization of the pH probe with early (*C*) or late (*D*) endosomal markers. Bars represent mean \pm S.E. of three independent experiments.

indicate that inhibition of MCOLN3 function strongly affects release of Ca²⁺ from endosomes.

MCOLN3 Is Required for Proper Endosomal Acidification—Release of Ca²⁺ has been linked to endosomal acidification. The suggestion is that the uptake of H⁺ into endosomes mediated by the vacuolar H⁺ pump must be balanced by Ca²⁺ efflux via endosomal calcium channels. Alternatively, Ca²⁺ release may be necessary to keep K⁺ and Cl⁻ channels open so that charge compensation can occur (11).

To evaluate the importance of Ca²⁺ in endosomal acidification, we compared the pH of early and late endosomes in cells preincubated for 1 h in a physiological buffer with normal (2 mM) or low (0.2 mM) Ca²⁺ concentration (Fig. 2). Measurement of endosomal pH was performed by simultaneous loading of cells with FITC-conjugated dextran (sensitive to pH) and Alexa Fluor 555-conjugated dextran (not sensitive to pH) for 10 min. Living cells were then analyzed by confocal microscopy 20 min or 1 h after the beginning of the loading (Figs. 2*A* and 3, *A* and *B*). The fluorescence ratio of green (FITC-dextran) to red (Alexa Fluor 555-dextran) is indicative of the luminal pH of the compartment (16). A curve constructed by measuring fluorescence ratios in permeabilized cells equilibrated with different calibration solutions (from pH 4 to pH 8) was made to correlate measured fluorescence ratio and absolute pH values (Fig. 3*C*).

Quantification of endosomal pH in cells incubated in normal Ca²⁺ buffer showed progressive acidification of the endosomal pathway, going from pH 5.80 (± 0.05 $n = 67$; where n indicates fields of cells) at 20-min incubation to pH 4.20 (± 0.05 $n = 67$) at 1-h incubation (Fig. 2*B*). Some acidification was also observed in cells incubated with low Ca²⁺ buffer, but the process was

significantly less efficient with pH 6.99 (± 0.18 $n = 64$) at 20-min incubation and pH 5.31 (± 0.03 $n = 58$) at 1-h incubation (Fig. 2*B*). In contrast, Ca²⁺ concentration did not affect internalization or trafficking of dextran along the endocytic pathway as no significant differences were observed in the colocalization of dextran with early (EEA1) and late (Lamp1) endosomal markers in cells incubated with 2 mM or 0.2 mM Ca²⁺ concentration (Fig. 2, *C* and *D*, and supplemental Fig. 4). Therefore, our data confirm that endosomal Ca²⁺ plays an important role in pH reduction in the endosomal pathway.

Given the reduced luminal Ca²⁺ release in cells depleted of MCOLN3, we assessed whether the inhibition of MCOLN3 function also has an effect on endosomal acidification. We have shown that MCOLN3 overexpression alters endosomal pH (10). As expected, expression of MCOLN3 DDKK dramatically decreased endosomal acidification both at early and late dextran internalization times (Fig. 3, *D* and *E*). At 20-min internalization endosomal pH was 5.65 (± 0.04 $n = 63$) in control (mock-infected) cells compared with pH 6.24 (± 0.19 $n = 37$) in cells expressing the DDKK mutant. At 1-h internalization the pH was 4.07 (± 0.06 $n = 49$) in control cells versus pH 5.61 (± 0.05 $n = 50$) in DDKK-expressing cells. In contrast, infection with a null virus did not have any effect on endosomal pH (Fig. 3, *D* and *E*). Depletion of endogenous MCOLN3 also reduced endosomal acidification (Fig. 3, *F* and *G*). At the early endosomal pathway the luminal pH was significantly increased in cells treated with MCOLN3 siRNA (pH 6.10 ± 0.07 $n = 79$) compared with cells transfected with nontarget siRNA (pH 5.51 ± 0.04 $n = 71$) (Fig. 3*F*). Increased pH in cells depleted of MCOLN3 was also observed at the late endosomal pathway in

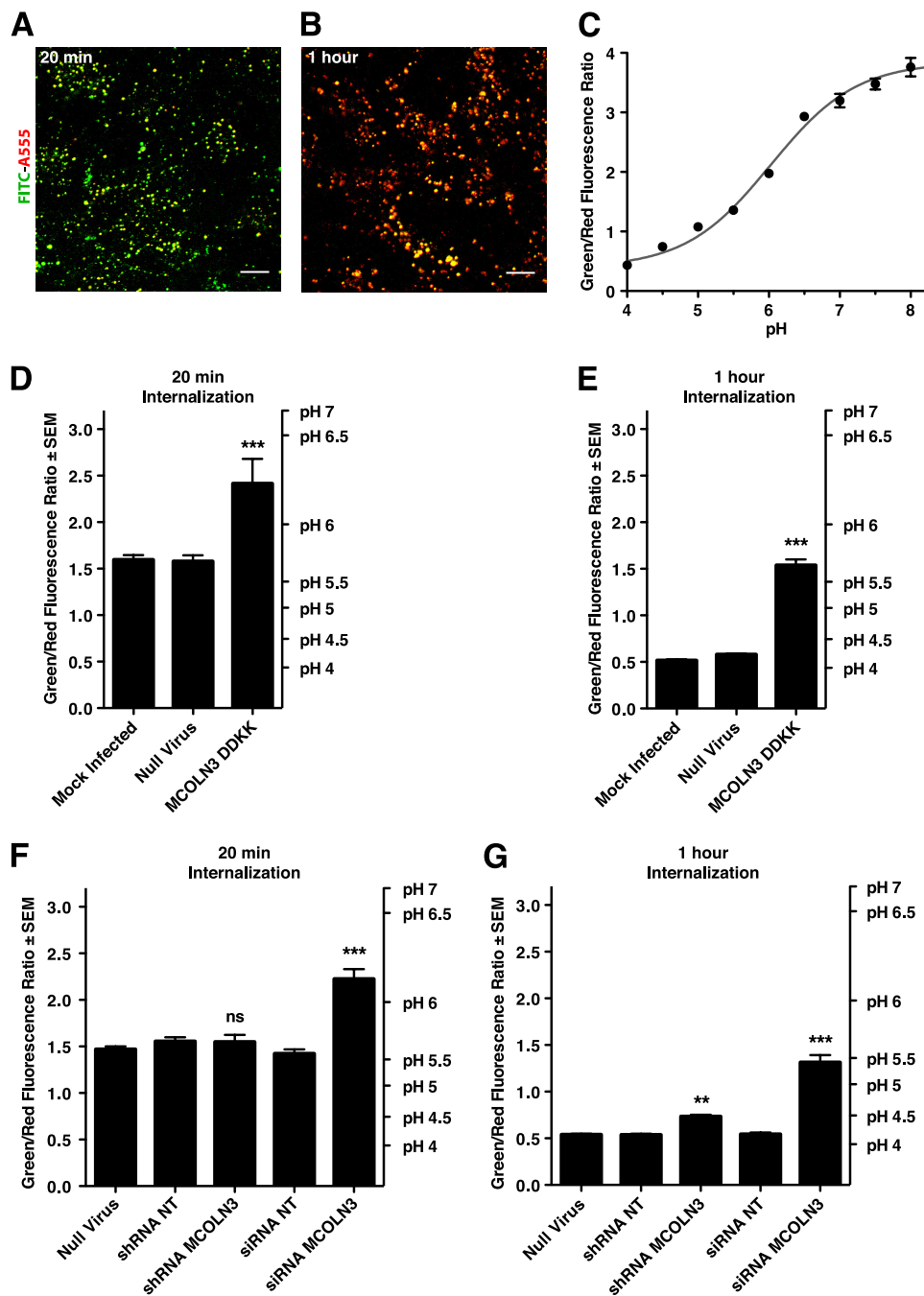


FIGURE 3. **Disruption of MCOLN3 function causes increased endosomal pH.** A and B, endosomal pH was measured by fluorescence ratio imaging at 20 min (A) or 1 h (B) after internalization of the probes. Scale bars, 10 μ m. C, calibration curve was constructed by calculating ratios in permeabilized cells equilibrated with calibration solutions. D–G, quantification of endosomal pH in cells expressing an inactive MCOLN3 mutant (D and E) or cells depleted of endogenous MCOLN3 (F and G) is shown. Bars represent mean \pm S.E. of three independent experiments. ***, $p < 0.001$; **, $p < 0.01$.

cells expressing siRNA against MCOLN3 ($\text{pH } 5.42 \pm 0.07$ $n = 65$) versus cells treated with control siRNA ($\text{pH } 4.18 \pm 0.07$ $n = 67$) (Fig. 3E). Depletion of MCOLN3 by shRNA did not cause a strong inhibition of endosomal acidification at the early internalization times, but the differences were significant at late internalization times (Fig. 3, F and G). This probably reflects the reduced accumulation of luminal Ca^{2+} in cells treated with MCOLN3 shRNA compared with cells treated with MCOLN3 siRNA (Fig. 1F) and may be a consequence of the less efficient depletion of endogenous MCOLN3 achieved by treatment with shRNA (supplemental Fig. 1). Taken together, our results indi-

cate that MCOLN3 is required for proper endosomal acidification.

*Defects in MCOLN3 Function Increase Endosomal Fusion—*Release of endosomal Ca^{2+} is known to be important for membrane trafficking. For example, release of luminal Ca^{2+} is required for the homotypic fusion of endosomes (17) and the heterotypic fusion of late endosomes with lysosomes (18). We assessed whether MCOLN3 function may be important for the regulation of fusion events between endosomes. To measure homotypic fusion of endosomes we developed an *in vitro* fusion assay. Briefly, one population of cells was incubated with

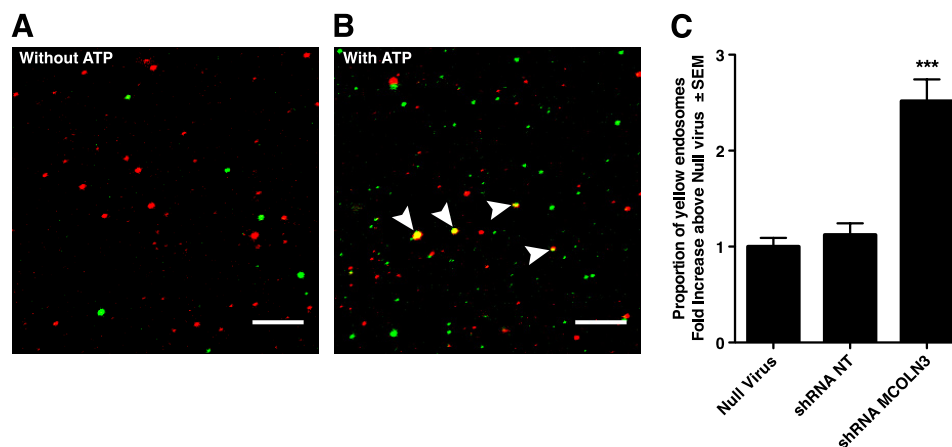


FIGURE 4. **MCOLN3 depletion leads to increased endosomal fusion.** *A* and *B*, endosomal fusion was quantified by confocal microscopy in the absence (*A*) or presence (*B*) of ATP. *Arrowheads* indicate fusion events. *Scale bars*, 10 μm . *C*, quantification of three independent experiments showing increased endosomal fusion in cells depleted of MCOLN3. ***, $p < 0.001$.

Alexa Fluor 488 EGF, and the other cells were incubated with Alexa Fluor 555 EGF for 15 min to label the early endosomal compartment. Time course internalization assays confirmed that at this time EGF mainly accumulated at early endosomes, showing a high degree of co-localization with the early endosomal marker EEA1 and low co-localization with the late endosomal-lysosomal marker LBPA (supplemental Fig. 5, *A* and *B*). Endosomes were then purified and subjected to an *in vitro* fusion assay. At the end of the incubation, endosomes were fixed on glass coverslips and analyzed by confocal microscopy. Endosomal fusion was quantified by measuring the proportion of yellow endosomes. Analysis of the purified endosomal fraction by Western blotting confirmed the presence of early endosomal markers, including Rab5 and transferrin receptor (supplemental Fig. 5C).

Fusion of early endosomes was virtually absent in control experiments performed without ATP ($0.70\% \pm 0.18$) whereas the percentage of endosomes that undergo homotypic fusion increased to almost 5% ($4.91\% \pm 0.83$) in the presence of ATP, thus confirming the specificity of the assay (Fig. 4, *A* and *B*). Interestingly, depletion of endogenous MCOLN3 significantly increased endosomal fusion. Quantification of three independent experiments revealed a 2.5-fold increase (2.52 ± 0.83 $n = 181$, where n represents fields of vesicles) in the number of fusion events in cells expressing MCOLN3 shRNA whereas no effect was observed after expression of the control nontarget shRNA (Fig. 4C).

Our data provide novel insight into the cellular function of endogenous MCOLN3. Most previous studies on MCOLN3 were based on the overexpression of the recombinant protein in different cell lines or in the analysis of a gain-of-function mutant of MCOLN3 (Va mutant). Only two studies have previously addressed the effect of depleting endogenous MCOLN3, finding alterations in autophagosome degradation and trafficking of EGFR from the plasma membrane to lysosomes (8, 10). Here, we show that MCOLN3 mediates release of Ca^{2+} from the lumen of endosomes. Inhibition of MCOLN3 function causes increased accumulation of luminal Ca^{2+} , and this accumulation has important consequences on endosomal acidification and membrane fusion. Therefore, our findings

explain the reported alterations of the endosomal pathway caused by defective MCOLN3 function.

Numerous *in vitro* and *in vivo* studies have established that the release of calcium from the lumen of endosomes and lysosomes plays a crucial role in membrane trafficking at the endocytic pathway (17, 18). Thus, for example, calcium efflux is required for triggering the final steps of membrane fusion. The increased endosomal fusion observed in the absence of MCOLN3 suggests that the abnormal accumulation of Ca^{2+} in endosomes might trigger the activation of alternative Ca^{2+} channels localized in this compartment, such as the two-pore channels (19, 20) (supplemental Fig. 6).

Recently, Samie *et al.* performed real-time quantitative RT-PCR analyses of mouse MCOLN3 expression patterns from 16 different adult mouse tissues (21). They found that MCOLN3 was expressed at low level in all of the tissues analyzed. Expression of MCOLN3 was higher in lymphoid (thymus and spleen) and kidney organs followed by colon and lung. In addition, our laboratory has detected expression of MCOLN3 in several human cell lines, including ARPE-19, HeLa, HEK293, and human fibroblasts.³ Therefore, MCOLN3 is probably present in most cell types, thus supporting the biological significance of the data presented in this study. The higher expression of MCOLN3 in certain tissues may indicate specific properties or requirements of the endosomal pathway in these specific cell types.

The important role played by endosomal Ca^{2+} in traffic through the endocytic pathway suggests that alteration of luminal Ca^{2+} may lead to disease. In agreement with this idea, it was recently described that cells from Niemann-Pick type C1 patients have altered calcium homeostasis, leading to the storage of sphingolipids and cholesterol at late endocytic compartments (22). In addition, mutations in MCOLN1, another member of the mucolipin family, result in mucopolipidosis type IV (MLIV), a lysosomal storage disorder characterized by severe neurological and ophthalmological defects (23). It has been proposed that defects on MCOLN1 function alter Ca^{2+} efflux

³ B. Lelouvier, J. A. Martina, and R. Puertollano, unpublished observations.

MCOLN3 Regulates Endosomal Calcium

from lysosomes thereby altering the fusion between late endosomes and lysosomes as well as lysosomal reformation (24). Our data reaffirm the importance of the luminal ionic composition of organelles in the endocytic pathway.

Acknowledgments—We thank Roberto Weigert for helpful discussions and suggestions. We also appreciate the editorial assistance of the National Institutes of Health Fellows Editorial Board.

REFERENCES

1. Di Palma, F., Belyantseva, I. A., Kim, H. J., Vogt, T. F., Kachar, B., and Noben-Trauth, K. (2002) *Proc. Natl. Acad. Sci. U.S.A.* **99**, 14994–14999
2. Kim, H. J., Li, Q., Tjon-Kon-Sang, S., So, I., Kiselyov, K., and Muallem, S. (2007) *J. Biol. Chem.* **282**, 36138–36142
3. Kim, H. J., Li, Q., Tjon-Kon-Sang, S., So, I., Kiselyov, K., Soyombo, A. A., and Muallem, S. (2008) *EMBO J.* **27**, 1197–1205
4. Xu, H., Delling, M., Li, L., Dong, X., and Clapham, D. E. (2007) *Proc. Natl. Acad. Sci. U.S.A.* **104**, 18321–18326
5. Cuajungco, M. P., and Samie, M. A. (2008) *Pflugers Arch.* **457**, 463–473
6. Grimm, C., Cuajungco, M. P., van Aken, A. F., Schnee, M., Jörs, S., Kros, C. J., Ricci, A. J., and Heller, S. (2007) *Proc. Natl. Acad. Sci. U.S.A.* **104**, 19583–19588
7. van Aken, A. F., Atiba-Davies, M., Marcotti, W., Goodyear, R. J., Bryant, J. E., Richardson, G. P., Noben-Trauth, K., and Kros, C. J. (2008) *J. Physiol.* **586**, 5403–5418
8. Kim, H. J., Soyombo, A. A., Tjon-Kon-Sang, S., So, I., and Muallem, S. (2009) *Traffic* **10**, 1157–1167
9. Zeevi, D. A., Frumkin, A., Offen-Glasner, V., Kogot-Levin, A., and Bach, G. (2009) *J. Pathol.* **219**, 153–162
10. Martina, J. A., Lelouvier, B., and Puertollano, R. (2009) *Traffic* **10**, 1143–1156
11. Gerasimenko, J. V., Tepikin, A. V., Petersen, O. H., and Gerasimenko, O. V. (1998) *Curr. Biol.* **8**, 1335–1338
12. Dunn, K. C., Aotaki-Keen, A. E., Putkey, F. R., and Hjelmeland, L. M. (1996) *Exp. Eye Res.* **62**, 155–169
13. Karacsonyi, C., Miguel, A. S., and Puertollano, R. (2007) *Traffic* **8**, 1404–1414
14. Lev, S., Zeevi, D. A., Frumkin, A., Offen-Glasner, V., Bach, G., and Minke, B. (2010) *J. Biol. Chem.* **285**, 2771–2782
15. Pryor, P. R., Reimann, F., Gribble, F. M., and Luzio, J. P. (2006) *Traffic* **7**, 1388–1398
16. Dunn, K., and Maxfield, F. R. (2003) *Methods Cell Biol.* **72**, 389–413
17. Yan, Q., Sun, W., McNew, J. A., Vida, T. A., and Bean, A. J. (2004) *J. Biol. Chem.* **279**, 18270–18276
18. Pryor, P. R., Mullock, B. M., Bright, N. A., Gray, S. R., and Luzio, J. P. (2000) *J. Cell Biol.* **149**, 1053–1062
19. Brailoiu, E., Churamani, D., Cai, X., Schrlau, M. G., Brailoiu, G. C., Gao, X., Hooper, R., Boulware, M. J., Dun, N. J., Marchant, J. S., and Patel, S. (2009) *J. Cell Biol.* **186**, 201–209
20. Calcraft, P. J., Ruas, M., Pan, Z., Cheng, X., Arredouani, A., Hao, X., Tang, J., Rietdorf, K., Teboul, L., Chuang, K. T., Lin, P., Xiao, R., Wang, C., Zhu, Y., Lin, Y., Wyatt, C. N., Parrington, J., Ma, J., Evans, A. M., Galione, A., and Zhu, M. X. (2009) *Nature* **459**, 596–600
21. Samie, M. A., Grimm, C., Evans, J. A., Curcio-Morelli, C., Heller, S., Slaugenhaupt, S. A., and Cuajungco, M. P. (2009) *Pflugers Arch.* **459**, 79–91
22. Lloyd-Evans, E., Morgan, A. J., He, X., Smith, D. A., Elliot-Smith, E., Silence, D. J., Churchill, G. C., Schuchman, E. H., Galione, A., and Platt, F. M. (2008) *Nat. Med.* **14**, 1247–1255
23. Bach, G. (2001) *Mol. Genet. Metab.* **73**, 197–203
24. Piper, R. C., and Luzio, J. P. (2004) *Trends Cell Biol.* **14**, 471–473